

Recent advances in metal triplet emitters with d⁶, d⁸ and d¹⁰ electronic configurations

Wai-Pong To,¹ Qingyun Wan,¹ Glenna So Ming Tong,¹ Chi-Ming Che^{1,2*}

¹State Key Laboratory of Synthetic Chemistry and Department of Chemistry, The University of Hong Kong, Pokfulam Road, Hong Kong SAR, People's Republic of China

² HKU Shenzhen Institute of Research and Innovation, Shenzhen, People's Republic of China

*Correspondence: cmche@hku.hk (C.-M. Che)

Abstract:

Basic research on the photophysical and photochemical properties of metal triplet emitters has been fueled by their practical applications in diverse areas including bioimaging, photocatalysis and organic light-emitting diodes (OLEDs). In addition to the extensively investigated Ru(II), Ir(III) and Pt(II) complexes, a wide range of luminescent Pd(II), Au(III)/Au(I), Re(I), Cu(I), W(VI)/W(0) and Mo(0) complexes have recently been revealed via the judicious choice of ligands to exhibit unique emissive excited states with a large range of radiative and nonradiative decay rate constants. Here, we provide an account of the design strategies of and recent advances on metal triplet emitters. Questions regarding future research in this field are presented.

Recent advances in luminescent transition metal complexes

The rapid growth of research on luminescent materials in recent decades has largely been driven by the diverse applications of these materials in various fields such as in OLEDs and chemo/biosensors. In particular, luminescent metal complexes have been attracting burgeoning interest because of the countless possible combinations of metal ions and ligands that could lead to different yet tunable spectroscopic and excited state properties. For second- and third-row transition metal complexes, phosphorescence is usually observed, which is attributed to the presence of a heavy metal atom that enhances spin-orbit coupling, leading to efficient intersystem crossing from singlet to triplet excited state manifolds upon photoexcitation. The presence of a heavy metal atom can also relax the spin-selection rule, allowing the radiative transition from T₁ to S₀ to occur. Accordingly, third-row transition metal complexes such as those with the commonly studied Re(I), Pt(II), Os(II) and Ir(III), have been extensively studied and found to display phosphorescence with lifetimes usually ranging from 0.1 to tens of microseconds after photoexcitation.[1-3] The nature of their

emissive triplet excited states highly depends on the electronic properties of the coordinated ligand(s). Structures of ligands often employed in the design of luminescent metal complexes are shown in Figure 1. Commonly observed excited states include MLCT (metal-to-ligand charge transfer), IL/LC (intraligand/ligand-centred), ILCT (intraligand charge transfer) and LLCT (ligand-to-ligand charge transfer) ones. Electronically excited metal complexes can undergo electron transfer and/or energy transfer with other molecules and their phosphorescence could be significantly perturbed by subtle changes in microenvironment particularly for those charge-transfer excited states, accounting for their numerous applications [4-6]. In recent years, substantial efforts have been devoted to developing photofunctional metal complexes based on earth-abundant metals including Fe, Cu, Zn, Zr, W and Ce and the results are encouraging [7-9]. In this article, recent advances on the design and applications of luminescent transition metal complexes are discussed.

Key Parameters of Triplet Emitters

An emitter with a high emission quantum yield is generally desired in almost all types of light-related applications. For efficient conversion of absorbed photons into emitted photons, two important parameters, the photoluminescence quantum yield (Φ_{PL}) and emission lifetime (τ), need to be optimized. These two parameters are related to the radiative decay rate constant (k_r) and non-radiative decay rate constant (k_{nr}) as follows:

$$\Phi_{\text{PL}} = \frac{k_r}{k_r + k_{nr}} \quad (1)$$

$$\tau = \frac{1}{k_r + k_{nr}} \quad (2)$$

For excited triplet emitters to display strong luminescence, it is of paramount importance for the emitter to possess a small k_{nr} and a comparatively large k_r . Strategies for increasing the k_r and suppressing the k_{nr} of mononuclear metal complexes are depicted in Boxes 1 and 2, respectively.

Box 1. Molecular Design Strategy for Increasing k_r

The radiative decay rate constant, k_r , is related to the transition dipole moment (\mathbf{M}) of the emitting state:

$$k_r(\tilde{\nu}) = \frac{8\pi^2 \eta^3 \tilde{\nu}^3}{3\epsilon_0 \hbar} |\mathbf{M}|^2 \quad (3)$$

For the triplet radiative decay rate, the transition dipole moment of the α -substate of the T_1 excited state (\mathbf{M}_T^α) is given by:

$$\mathbf{M}_T^\alpha = \sum_{j \in x,y,z} \left| \sum_m \frac{\langle T_1^\alpha | H_{SOC} | S_m \rangle}{E(S_m) - E(T_1)} \mathbf{M}_{S_m,j} \right|^2 \quad (4)$$

where $\mathbf{M}_{S_m,j}$ is the j -axis projection of the $S_m \rightarrow S_0$ transition dipole moment, $E(T_1)$ and $E(S_m)$ are the energies of the T_1 and m^{th} singlet (S_m) excited states, and $\langle T_1^\alpha | H_{SOC} | S_m \rangle$ is the spin-orbit coupling (SOC) matrix element between the T_1 α -substate and S_m . Thus, to obtain a large k_r , three critical parameters need to be considered:

- (1) The SOC matrix element $\langle T_1^\alpha | H_{SOC} | S_m \rangle$ should be large, which could be attained by having a large metal character in the emitting excited state and/or metals with a large SOC constant such as the third-row transition metals (e.g., Ir, Pt and Au).
- (2) The S_m excited state should be close-lying to the T_1 excited state such that $E(S_m) - E(T_1)$ is small.
- (3) The singlet excited state that lends intensity to the $T_1 \rightarrow S_0$ transition should have a large $\mathbf{M}_{S_m,j}$.

The T_1 of most d^6 Ir(III) complexes has a large metal orbital character arising from MLCT (metal-to-ligand charge transfer) and hence, it exhibits a large $k_r \sim 10^5 - 10^6 \text{ s}^{-1}$, while the T_1 of Pt(II) complexes usually involves MLCT (minor) mixed with a ligand-based excited state (major), leading to a smaller k_r ($\sim 10^4 - 10^5 \text{ s}^{-1}$) [10]. In addition, for an efficient ISC process, the d-orbitals in both the singlet and emitting T_1 excited states have to be of different orientations. For the Ir(III) complex in an octahedral coordination environment, the non-bonding $d\pi$ -orbitals are close-lying, while the d-orbital splitting in the Pt(II) complex is larger. Therefore, the energy gap between the coupling singlet excited state and T_1 excited state is usually larger in Pt(II) than in Ir(III) complexes. An efficient way to enhance the k_r of Pt(II) complexes is to increase the \mathbf{M} of S_n . In our study on tetradentate Pt(II) complexes, **Pt-1** and **Pt-2** complexes having a fused O⁺N moiety usually exhibit k_r of 10^4 s^{-1} (Figure 1a). As the transition dipole moment density has significant contributions from the pyridine rings,

amino groups are added to the pyridine ring (**Pt-3** and **Pt-4**) to increase M (Figure 1b). Based on DFT/TDDFT calculations, the k_r values of **Pt-3** and **Pt-4** are enhanced to $1.07\text{--}1.25 \times 10^5 \text{ s}^{-1}$.

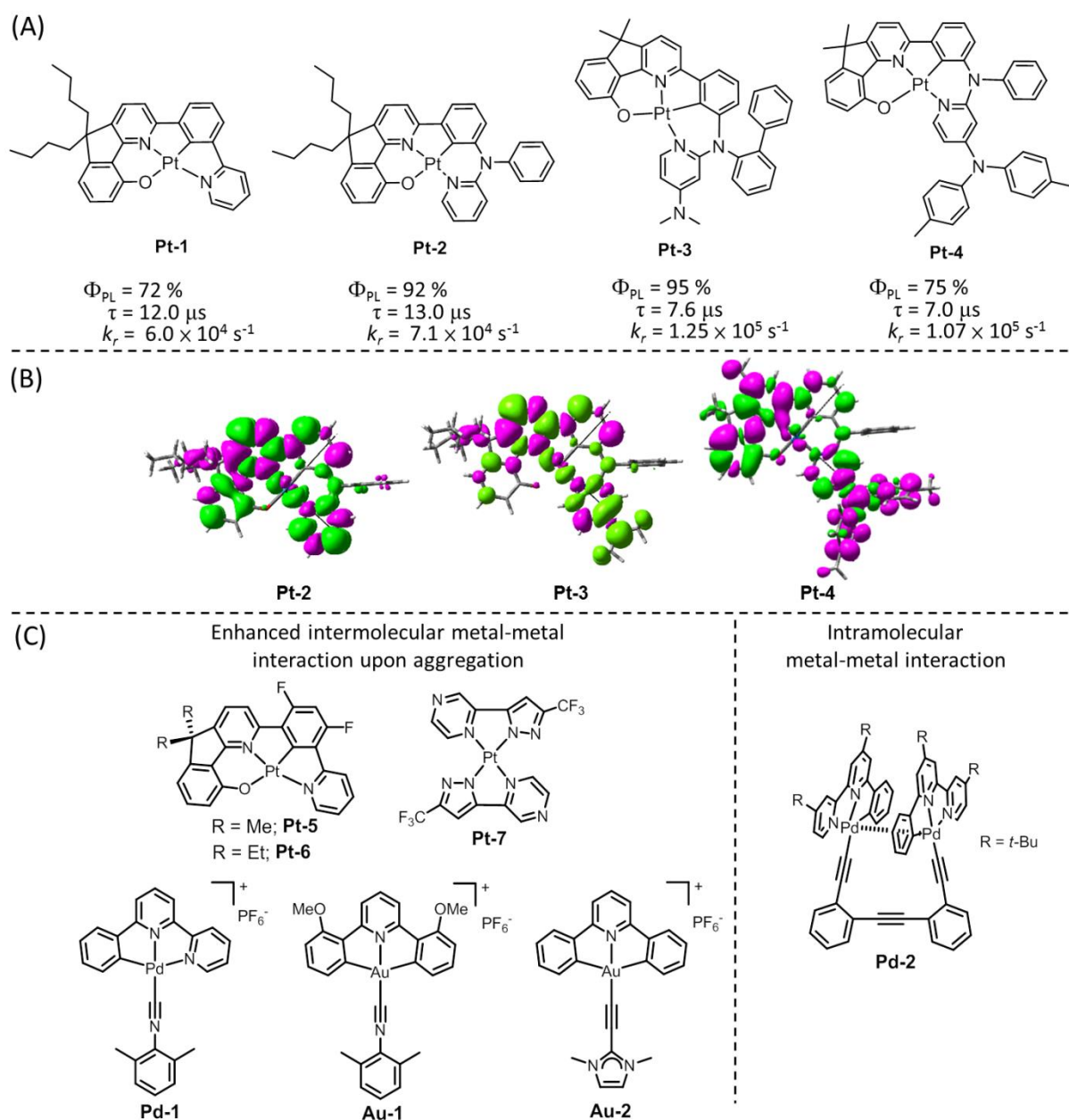


Figure 1 Design of d^8 metal complexes with enhanced k_r . (A) Structures of **Pt-1–Pt-4** complexes. (B) Key transition dipole moment density of the S_1 of the **Pt-2–Pt-4** complexes. (C) Examples of complexes exhibiting enhanced k_r due to the enhanced metal contribution in the emissive excited state.

Box 2. Molecular Design Strategy for Suppressing k_{nr}

There are two main approaches to suppressing k_{nr} . The first one is destabilization of close-lying deactivating excited states. d^8 transition metal complexes have a vacant $d\sigma^*$ orbital, which could be thermally accessible if this orbital is low-lying, such as the $4d_{x^2-y^2}$ orbital of electrophilic Pd(II) complexes with a planar coordination geometry. Population of this orbital could lead to elongation of the metal–ligand bond, resulting in large structural distortion and providing a facile non-radiative decay pathway. The use of strong σ -donor ligand(s) could destabilize the $d\sigma^*$ orbital such that it becomes thermally less accessible, thereby suppressing k_{nr} [11,12]. The second approach is minimizing the structural distortion of the emitting excited state relative to the ground state. The use of a rigid, multidentate ligand scaffold and/or a ligand with extended π -conjugation is an effective approach to minimizing excited state structural distortion [13-25].

Both methods are successful in the design of metal triplet emitters displaying high photoluminescence quantum yield (Φ_{PL}). For instance, Pt(II) and Pd(II) complexes with tetradentate ligands having deprotonated C donor(s) exhibit high Φ_{PL} values of >90% in thin films and up to 47% in solutions [13-18]. Notably, the tetradentate Pd(II)-O^NC^N complexes with a fused O^N chelating moiety (e.g. **Pd-3** in Figure 1c) are the first examples of nonporphyrin-type Pd(II) complexes showing strong, high energy phosphorescence in the blue-green spectral region at room temperature. With the use of rigid tetradentate ligands, the resulting d^8 metal emitters displayed excellent performance in OLEDs with EQEs of over 27% and 16% for tetradentate Pt(II) and Pd(II) emitters, respectively [16,18,26].

Another example of significant suppression of k_{nr} was demonstrated for gold(III) complexes with extended π -conjugation and fluorene-functionalized pincer-type C^NC ligands. These gold(III) complexes exhibit enhanced photoluminescence quantum yield ($\Phi_{PL} = 11\text{--}58\%$) attributable to effective suppression of k_{nr} to $<10^4 \text{ s}^{-1}$ (e.g. **Au-1**, **Au-2** in Figures 1a and 1b) [19,20]; the corresponding k_{nr} without extended π -conjugation is $>10^6 \text{ s}^{-1}$ [12,27]. With the high Φ_{PL} induced by the low k_{nr} , the OLED fabricated with the fluorene-functionalized C^NC gold(III) complex showed an EQE of 20.31%, which is the first Au(III) phosphorescent OLED with an EQE over 20% [28].

Hexakis(arylisocyanide) W(0) complexes exhibit a >10-fold increase in Φ_{PL} after appending an aryl substituent onto the isocyanide ligand [21]. The Mo(0) complex supported by *t*-butyl-substituted diisocyanide ligands (**Mo-1**) exhibits Φ_{PL} ~9-fold that of the complex with

methyl-substituted diisocyanide ligands (**Mo-2**) due to the suppression of k_{nr} by an order of magnitude attributed to enhanced structural rigidity of the complex induced by steric hindrance [22].

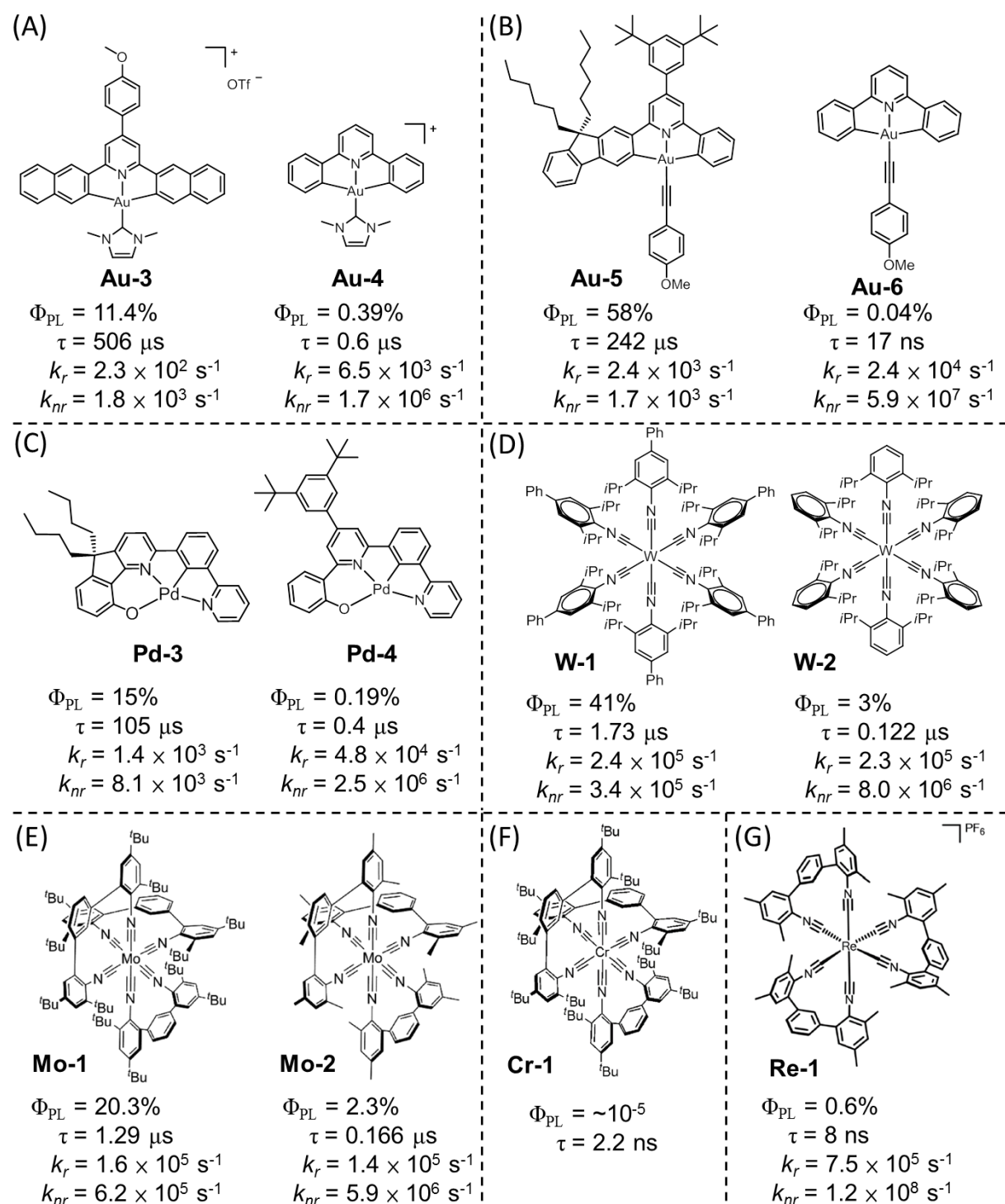


Figure 1 Ligand design for improving emission quantum yields. (A)-(D) Examples of metal complexes showing effective suppression of k_{nr} upon ligand modification. (E)-(G) Examples of complexes supported by bidentate diisocyanide ligands.

^{1/3}MMLCT and Intraligand Excimeric Excited States with Enhanced k_r

Because of the planar geometry with an open axial site (defined as the z-axis), d⁸ metal complexes are prone to form dimers/aggregates in the ground state or excimers in the excited state through intermolecular metal-metal and ligand-ligand interactions, giving rise to ^{1/3}MMLCT (metal-metal-to-ligand charge transfer) excited states in the cases of Pt(II) and Rh(I) systems [29]. In 1990 and 1991, Gliemann, Miskowski and coworkers reported and assigned the $d\sigma^*(Pt-5d_{z^2}) \rightarrow \pi^*$ transition of [Pt(bpm)(CN)₂] (bpm = 2,2'-bipyrimidine) and [Pt(bpy)(CN)₂] (bpy = 2,2'-bipyridine) in the solid state, respectively [30-32]. MMLCT emission of a discrete Pt(II) system in solution was first observed in a guanidine-bridged binuclear Pt(II) complex [33]. The MMLCT excited states exhibit a significant increase in metal character coming from the nd_{z²} orbital, and therefore a much larger k_r . Indeed, the ³MMLCT emission of discrete binuclear Pt(II) complexes with short Pt-Pt contacts such as Pt(II) amidinate dimers and Pt(II) 2-mercaptobenzimidazole dimers [34,35], is documented to have k_r values of 10⁵-10⁶ s⁻¹. We have reported that Pt(II)-O^{^N^C^N} complexes have a greatly shortened τ in neat film compared to that in solution owing to the enhanced k_r (close to 100-fold for **Pt-5** and **Pt-6**; Box 1, Figure 1c), accounting for the low efficiency roll-off (<5%) of the as-fabricated OLED [26]. DFT/TDDFT calculations revealed that intermolecular interactions in the solid state lead to the formation of a ³MMLCT excited state with an emission energy red-shifted from that of the monomer. Lin, Chou and Chi reported the fabrication of high-performance near-infrared OLEDs based on planar Pt(II) complexes. The solid-state thin film of **Pt-7** (Box 1, Figure 1c) exhibits intense NIR emission with an emission peak maximum at ~740 nm and high Φ_{PL} reaching 81% with a very large k_r of 2.59×10^6 s⁻¹, where the emission has been assigned to ³MMLCT [36]. Increasing k_r by increasing the metal character in the emissive excited state has also been demonstrated for Pd(II) complexes. We reported that cyclometalated Pd(II) isocyanide complexes (**Pd-1**; Box 1, Figure 1c) could undergo kinetically controlled supramolecular polymerization to form aggregates exhibiting ³MMLCT emission with a k_r of 6.22×10^5 s⁻¹ [37], which is significantly larger than the typical k_r value of 10³ s⁻¹ observed for Pd(II) complexes emitting from ligand-centered excited states. The binuclear, cyclometalated Pd(II)-alkynyl complexes with an intramolecular Pd-Pd contact of ~3.2–3.4 Å reported by Lu also exhibit strong emission with λ_{max} of 630–655 nm and k_r ranging from 1.5 – 2.4×10^5 s⁻¹, an example of which

is **Pd-2** in Box 1 Figure 1c. Their emissive excited states were suggested to have significant MMLCT parentage by TD-DFT calculations [38].

Au(III) ions are more electrophilic than Pd(II), rendering the formation of the MMLCT excited state in the UV-visible spectral region formidable. In our recent work, we found weak intermolecular bonding interactions between two cyclometalated Au(III) isocyanide and allenylidene complexes (**Au-1**, **Au-2**; Box 1, Figure 1c) in the excited states. These Au(III) complexes undergo supramolecular polymerization to give polymeric Au(III) species displaying a metal-perturbed $^3[\pi-\pi]^*$ excited state with k_r values of $1.5\text{--}2.1 \times 10^4 \text{ s}^{-1}$ [39], which are slightly greater than the k_r of $\sim 10^3 \text{ s}^{-1}$ for phosphorescent Au(III) complexes in discrete monomers exhibiting a triplet ligand-centered excited state.

Switching the Emission Mechanism to TADF

Since the works of Yersin and Adachi applying the mechanism of TADF emission in OLEDs [40,41], there has been an increase in the efforts to develop TADF materials for triplet exciton harvesting. For TADF emitters, the triplet excitons could be converted into singlet excitons by reverse ISC with the help of thermal activation, provided that the singlet-triplet energy gap (ΔE_{ST}) is small. Within a three-state model where the S_1 and T_1 excited states are in fast thermal equilibrium, the average τ is given by:

$$\tau = \frac{3 + \exp\left(-\frac{\Delta E_{ST}}{k_B T}\right)}{3k^P + k^F \exp\left(-\frac{\Delta E_{ST}}{k_B T}\right)}$$

where k^F and k^P are the fluorescence and phosphorescence decay rate constants, respectively ($k^P = k_r^P + k_{nr}^P$ and $k^F = k_r^F + k_{nr}^F$); k_B is the Boltzmann constant; and T is the temperature.

The singlet radiative decay rate constant (k_r^F) is much larger than the triplet radiative decay rate constant ($k_r^F > 10^7 \text{ s}^{-1}$ and $k_r^P \leq 10^6 \text{ s}^{-1}$) due to the spin-selection rule. Thus, a judicious molecular design to give a small ΔE_{ST} could give rise to emitters with τ in the submicrosecond regime. Yersin reported a variety of Cu(I) and Ag(I) complexes exhibiting high Φ_{PL} with emission origin assigned to TADF [42,43]. Recently, Thompson reported a family of carbene-Cu(I)-amide complexes displaying Φ_{PL} up to >99% and τ of $\sim 2\text{--}3 \mu\text{s}$ [44]. By employing a symmetry-based strategy for increasing the transition dipole moment of the emitting state of Cu(I) complexes, Yersin reported a binuclear Cu(I)-TADF emitter showing a τ of $1.2 \mu\text{s}$, which is much shorter than those of Cu(I)-TADF emitters with similarly small

ΔE_{ST} [45]. In 2017, Bochmann, Credginton and Linnolahti reported the first examples of Au(I) TADF emitters and their use in OLEDs (EQE up to ~27%) [46]. One of these complexes (**Au-7**) exhibits a Φ_{PL} of 83% in thin films with lifetime $< 1\mu s$ [47], which is ascribed to the small ΔE_{ST} values of ~ 300 and $\sim 800\text{ cm}^{-1}$ for the orthogonal and coplanar molecular conformations respectively [48]. Vacuum-deposited OLEDs fabricated with **Au-7** showed maximum EQEs of up to 26.9% [47]. Other metal complexes could also exhibit efficient TADF properties. Li reported tetradentate [Pd(N[^]C[^]C[^]N)] complexes displaying TADF in addition to ³IL phosphorescence with Φ_{PL} of up to 77% at room temperature [49,50]. For Au(III) complexes, Bochmann mentioned the possible involvement of TADF in a study on pyrazine-based pincer Au(III) complexes [51]. We found that cyclometalated Au(III)-C[^]N[^]C complexes with aryl or arylacetylidate ligands could display TADF with $\tau < 2\mu s$ and Φ_{PL} of up to 79% and 88% in solution and thin films, respectively, at room temperature (**Au-11-Au-14**) [52,53]. Notably, their k_r values on the order of $10^5\text{--}10^6\text{ s}^{-1}$ are much higher than the values of 10^3 s^{-1} generally observed for the phosphorescence of Au(III) complexes. In this case, a spatially separated donor-acceptor (D–A) molecular architecture is employed so that the lowest singlet and triplet excited states are dominantly ^{1,3}LLCT in character (LLCT = ligand-to-ligand charge transfer). The use of a C[^]N[^]C ligand with a high-energy ³IL excited state ($E_{0,0} > 2.6\text{ eV}$) is also crucial for the ^{1,3}LLCT excited states to become the lowest-lying states from which emission can occur. Based on DFT/TDDFT calculations and variable-temperature emission lifetime measurements, the ΔE_{ST} of these Au(III) emitters has been estimated to be $< 500\text{ cm}^{-1}$, which is small enough for efficient TADF to occur at room temperature. A high EQE of 23.4% and an efficiency roll-off down to 1% have been realized in OLEDs fabricated with these pincer Au(III) TADF emitters. Very recently, we reported a class of robust tetradentate Au(III) TADF emitters (**Au-15-Au-16**) exhibiting Φ_{PL} up to 94% and τ down to 0.62 μs [54]. OLEDs fabricated with these emitters showed EQEs up to 25% and operational lifetimes (LT_{95}) up to 5280 hours at 100 cd m^{-2} , the latter of which is at least 10 times better than that achieved with pincer gold(III) emitters [53, 55], affirming the practicability of tetradentate Au(III)-TADF emitters in OLEDs. By employing a similar design strategy, our group synthesized the first example of a metal-TADF emitter based on an earth-abundant 3rd-row transition metal, tungsten [56]. In this work, the W(VI) Schiff base dioxo complex **W-5** with a D–A–D molecular scaffold was found to exhibit excited states with mixed ILCT/LMCT character. Compared with the unsubstituted W(VI) complex **W-4** which exhibits typical long-lived emission with Φ_{PL} of 28% and τ of

222 μs , the presence of di-*p*-tolylamine substituents on the phenoxide moiety accounts for the drastic increase in Φ_{PL} to over 80% together with the greatly shortened τ of ~ 2.0 μs in thin film. The k_r of this complex is $4.2 \times 10^5 \text{ s}^{-1}$, which is *more than 300-fold larger* than that of the unsubstituted complex, and comparable to the k_r of W(0) hexakis(aryl isocyanide) complexes exhibiting $^3\text{MLCT}$ emission reported by Gray [21]. DFT calculations have revealed that the ΔE_{ST} of **W-5** is $\sim 1000 \text{ cm}^{-1}$, which is sufficiently small for TADF to be operative in this complex at room temperature.

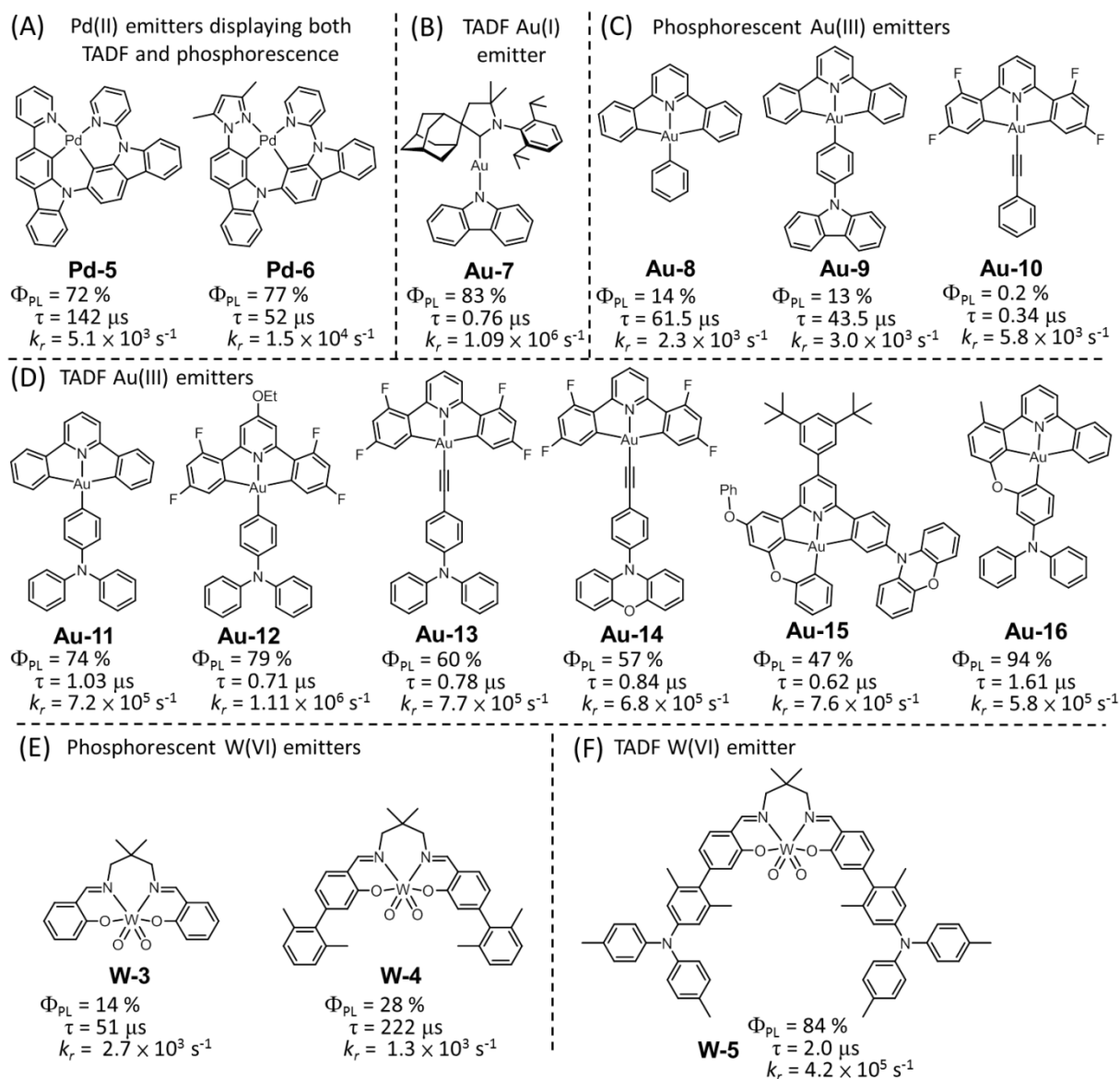
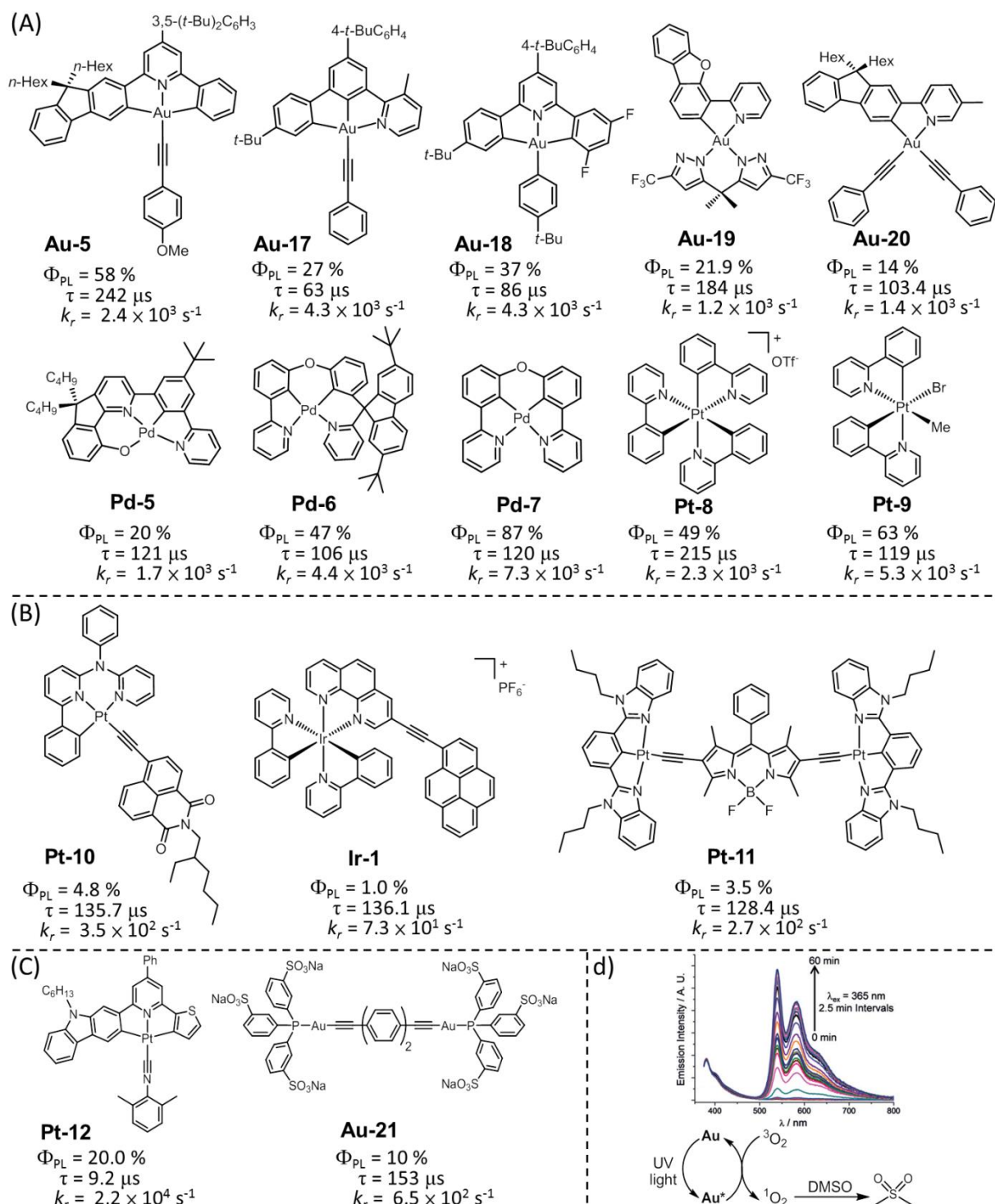


Figure 2 Examples of (A) Pd(II), (B) Au(I), (C)-(D) Au(III) and (E)-(F) W(VI) emitters exhibiting phosphorescence and TADF. Comparison between the structures of phosphorescent and TADF Au(III) complexes (compare (C) and (D)) and W(VI) complexes (compare (E) and (F)) revealed that TADF were achieved when strongly electron-donating amino-substituents (e.g. diarylamine, phenoxazine) were installed on the ligand. The emission

data of **Pd-5** were measured in a PMMA thin film, and those of **Pd-6** were measured in degassed CH₂Cl₂. The emission data of Au(III) complexes were collected in degassed toluene, while those of W(VI) complexes were collected in mCP thin films.

Long-Lived Triplet Excited States with Lifetimes over Tens of Microseconds

Triplet emitters with long excited state lifetimes ($> 100 \mu\text{s}$) are useful in bimolecular photocatalysis and in sensitizing triplet-triplet annihilation for energy up-conversion and energy transfer for energy down-conversion. Excited states with $\tau > 100\mu\text{s}$ theoretically result in a better efficiency of bimolecular reactions than that achieved with species such as [Ru(bpy)₃]²⁺ and [Ir(ppy)₃] with lifetimes of just a few microseconds. As the quenching efficiency of the excited state is correlated to τ , sensors with longer τ would display a higher sensitivity in sensing. To attain a long-lived excited state, both k_{nr} and k_r must be small. As metal parentage in a triplet excited state would increase k_r , an excited state with a predominant ligand character should have a small k_r . A strategy to achieve this is to employ electrophilic metal ions which have a minute contribution to the frontier MOs of the metal complex. Due to the electrophilicity of Au(III), Pd(II), Pt(IV) and W(VI) ions, their complexes display long-lived, ligand-centered phosphorescence with high quantum yields and lifetimes $> 50 \mu\text{s}$ (Figures 2a, 2e, and 3a) [17-20,56,57,58-61]. The pincer Au(III) and [Pd(O[^]N[^]C[^]N)] complexes with τ over $100 \mu\text{s}$ exhibit two-photon absorption, undergoing excited state energy transfer to achieve energy up-conversion and down-conversion, the latter of which has been utilized in phosphor-sensitized fluorescent OLEDs with EQEs reaching 14.3% [18]. These [Pd(O[^]N[^]C[^]N)] complexes also catalyzed photoinduced [2+2] styrene cycloaddition in a shorter reaction time and with higher product yields than those achieved with [Ir(ppy)₃] [18].



Another strategy is to conjugate an organic moiety with low-energy triplet excited state to a 2nd/3rd row transition metal complex so that the ISC from the singlet to triplet excited state is facilitated by the metal, while the observed emission comes from the low-energy triplet excited state of the organic moiety. Castellano and Zhao reported a panel of Ru(II), Pt(II) and Ir(III) complexes with ligands containing pyrene, naphthalimide and borondipyrromethene (Bodipy) (Figure 3b) [62,63]. These complexes exhibit orange to NIR phosphorescence with lifetimes over 50 μ s and were found to be efficient photosensitizers for energy up-conversion. The long-lived triplet excited state of metal complexes also enables efficient photosensitization of singlet oxygen and hence rapid depletion of dissolved oxygen under ambient light. In 2012, we found that the emission intensity of the Pt(II) complex **Pt-12** increased by 10 times upon standing under ambient light in aerated DMSO (Figure 3c) [64], which was attributed to the reaction between photogenerated singlet oxygen and DMSO that formed dimethyl sulfone leading to depletion of dissolved oxygen in the solution.

This phenomenon has recently been exemplified by Lu, who coined the term “photoactivated phosphorescence” [65]. Photoexcitation of an aerated DMSO solution containing **Au-21** (Figures 3c,d) resulted in photochemical depletion of dissolved oxygen in the solution, and hence, the phosphorescence of the Au(I) complex was gradually enhanced upon light excitation. This strategy has also been employed to achieve TTA photon up-conversion using Pt(II) octaethylporphyrin as a sensitizer in aerated DMSO solution [66]. By using the same sensitizer and a polymeric gel of poly(N-vinyl-2-pyrrolidone) as a photochemically deoxygenating matrix, photowriting of phosphorescence images onto the gel was realized, and the images were self-erased upon diffusion of oxygen into the matrix [67]. Photoactivated phosphorescence 3D images have also recently been achieved in DMSO with Pt(II) porphyrins [68].

Supramolecular d⁸ Metal Emitters

The planar geometry of d⁸ metal complexes facilitates intermolecular contacts leading to changes in emission properties such as k_r , k_{nr} and τ upon dimerization and/or aggregation. The inter/intramolecular interactions of d⁸ metal complexes are usually weak and significantly perturbed by external stimuli, which has become a useful strategy in developing supramolecular materials with wide applications in sensing, catalysis and bioimaging [69,70]. Reversible switching between monomer emission and MMLCT emission due to external stimuli or subtle changes in the local environment of supported Pt(II) complexes on silica/Nafion was realized as early as 2003 [71]. We recently reported that aggregates derived from Pt(II) and Pd(II) complexes are highly dependent on the counter anions [37,72]. The ‘cation-anion’ electrostatic interaction guides pincer d⁸ metal complexes to undergo supramolecular polymerization from a kinetically trapped metastable aggregate state to a thermodynamically stable aggregate state, during which a change in the excited state from the mixed ^{1/3}IL and ^{1/3}MLCT to ^{1/3}MMLCT appears. Yam and coworkers reported the control on the pathway complexity for a co-assembled system made by d⁸ Pt(II) complexes and covalent poly(ethylene glycol)–poly(acrylic acid) during seeded supramolecular polymerization to fabricate a supramolecular heterojunction [73]. De Cola and coworkers reported an amphiphilic luminescent platinum(II) complex which forms two kinetic aggregates and a thermodynamic self-assembly product with different emission properties [74]. By controlling the aggregation pathway, a ‘living’ crystallization-driven self assembly has been realized for such a Pt(II) complex reported by Manners and coworkers [75]. A supramolecular photocatalyst formed from discrete binuclear Pt(II) complexes shows a ³MMLCT excited state capable of sensitizing the generation of ¹O₂ for oxidation of secondary amine to imine [76]. Its photocatalytic activity can be switched off with the addition of Zn²⁺ and switched on again by adding 2,2':6',2''-terpyridine attributed to the reversible switching on/off of the ³MMLCT excited state. Conductive nanowires with infinite Pt(II)···Pt(II) chains formed by self-assembly of Pt(II) complexes were used to prepare organic light-emitting field-effect transistors (OLE-FETs) [77,78]. A submicrometer wire of a cyclometalated Pt(II) isocyanide complex displayed brighter ³MMLCT emission at the ends of the wire than from the wire body, suggesting application as an optical waveguide [77].

Clam-shell or “butterfly” binuclear Pt(II) pyrazolate complexes such as **Pt-13–Pt-15** show short intramolecular metal-metal distances (3.49 Å for **Pt-13**; Figure 4) [79] and display ³IL phosphorescence in solution. A subsequent work by Thompson found that the intramolecular metal-metal interaction can be modulated by varying the bulkiness of the bridging pyrazolate

ligand.[80] With structural modification of the C^N ligand, **Pt-16** (Figure 4) displays two excited states upon photoexcitation, with one having mixed ³LC/³MLCT characters and the other having ³MMLCT character due to the shortened intramolecular metal-metal distance in the excited state [81]. Since the population ratio of these two excited states could be perturbed by the molecule's local environment, the dual emission of these complexes has been utilized for sensing of viscosity and temperature [82].

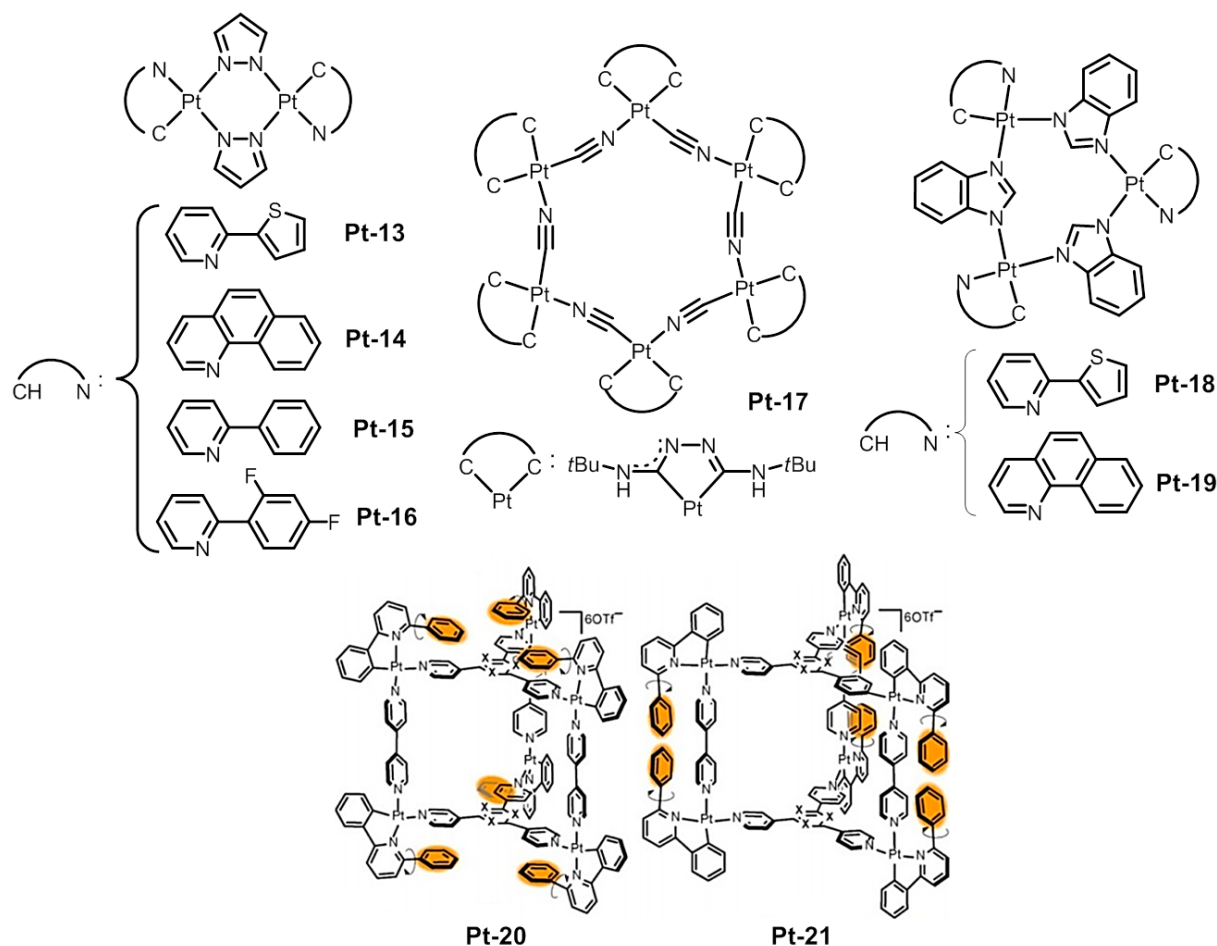


Figure 4 Structures of multinuclear Pt(II) complexes and cages assembled with Pt(II) complexes. Reprinted (adapted) with permission from [86]. Copyright 2019 American Chemical Society.

Host-guest interactions can affect the excited state manifold, and the effect of such interaction is amplified in oligomeric and/or macrocyclic structures. The first example of a luminescent Pt(II) macrocycle **Pt-17** supported by carbon-donor ligands was reported in 1998 [83]. By employing deprotonated 2-phenylpyridine as the cyclometalating ligand and benzimidazole as the bridging ligand, phosphorescent cyclometalated Pt(II) cyclic trimers **Pt-18** and **Pt-19** were prepared by a self-assembly reaction [84]. Stang and Huang prepared highly fluorescent

tetragonal Pt(II) metallacages supported by tetra-(4-pyridylphenyl)ethylene [85]. The emission color of these cages was readily tuned by varying the fraction of hexane in CH₂Cl₂. The emission color of one of these cages changed from yellow to blue to cyan upon increasing the hexane content from 0% to 90%, which was accompanied by an increase in Φ_{PL} from 23.2% to 60.6%. A recent work by Hor, Huang and co-workers described two triangular metallaprisms assembled with Pt(II) complexes (**Pt-20**, **Pt-21**; Figure 4) that display redshifted emission in CH₂Cl₂/hexane mixtures ascribable to the rigidification of phenyl rings at the Pt-corners [86]. Interested readers are referred to the review articles by Mukherjee, Cook and Stang for further information on metallacycles and metallacages [87,88].

The sensitivity of triplet excited states to the local chemical environment and stimuli enables phosphorescent metal complexes to be used for bioimaging and sensing [4,89], but the sensitivity and selectivity are more prominent for those planar complexes with open coordination sites. Transition metal complexes with planar structural motifs can bind with DNA via intercalation, which leads to emission changes that provide information about specific nucleic acid structures such as DNA mismatches. The molecular light switch-on effect was coined by Barton and others who developed Ru(II) and Rh(III) complexes for nucleic acid recognition, which are capable of recognizing single base mismatches in DNA duplexes with high specificity and affinity (Figure 5a) [90,91]. Cyclometalated Pt(II) complexes have also long been known to form emissive intercalating adducts with nucleic acids [92]. Due to the different spatial geometries of nucleobases in dsDNA and dsRNA, the selective formation of exciplex emission arising from π -electronic interactions between the triplet excited state of Pt(II) complexes and the nucleobase of DNA has been recently demonstrated and exploited for differentiating dsDNA and dsRNA [93]. Pt(II) complexes with functionalized NHC ligand were shown to differentiate cancer cells with different levels of mismatch repair capacity and to differentiate colon tumor tissue from normal tissue (Figure 5b) [94]. The microsecond time regime of phosphorescence allows the use of a time-gated technique for improving the signal-to-noise ratio in cell imaging by distinguishing it from fluorescence [95,96]. Metal complexes exhibiting dual fluorescence-phosphorescence have also been utilized as self-referenced ratiometric sensors for dissolved oxygen levels, which were used for identifying hypoxia in cells and tissues [97,98]. Che and coworkers showed that a pyrazole-functionalized pincer Pt(II) complex that aggregates in low-pH environment could accumulate in acidic lysosomes, leading to ³MMLCT emission [99]. A class of Pt(II)

terpyridyl complexes studied by Yam undergo self-assembly to give $^3\text{MMLCT}$ emissions, which has been harnessed for sensing of biological substances [100-102]. Selective detection of human serum albumin (HSA) by the $^3\text{MMLCT}$ emission from Pt(II) aggregates has been achieved through the FRET (Förster resonance energy transfer) in Pt(II) complex-polymer co-assemblies [103].

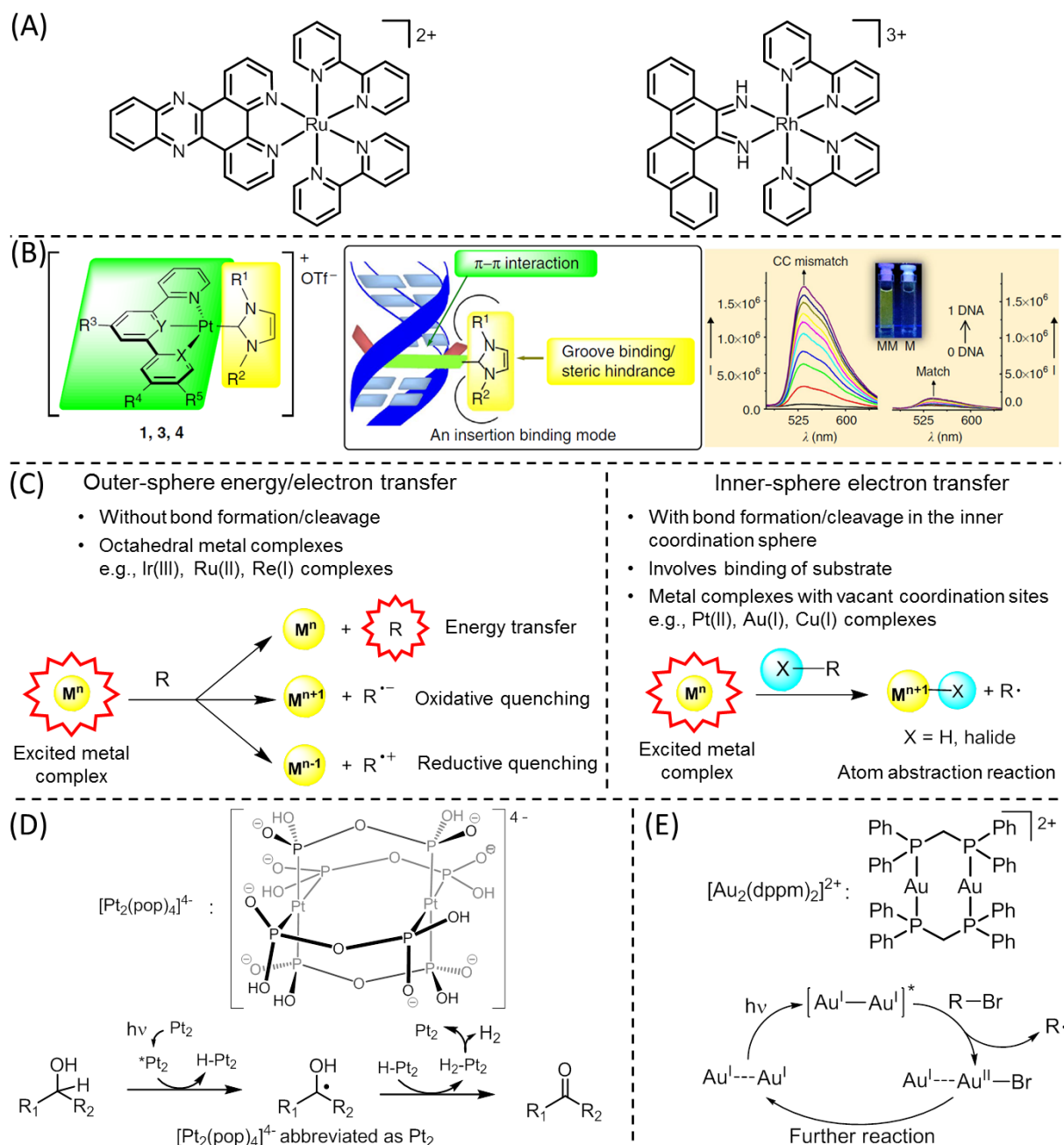


Figure 5 Chemical structures and schemes related to biologically active metal complexes and photocatalysis. (A) Rh(III) and Ru(II) complexes for nucleic acid recognition reported by Barton. (B) Pt(II) NHC complexes displaying different emission responses toward mismatched and matched DNA. Image reproduced with permission from [94]. (C) Difference

between outer-sphere and inner-sphere mechanism in photocatalysis. Proposed reaction pathway for (D) photodehydrogenation of alcohols by $[\text{Pt}_2(\text{pop})_4]^{4+*}$ and (E) halogen atom abstraction by $[\text{Au}_2(\text{dppm})_2]^{2+*}$. Image reproduced with permission from [106].

Excited State Inner-sphere Substrate Binding and Activation

Triplet emitters can function as strong one-electron donors and/or one-electron acceptors as exemplified by phosphorescent Ru(II) and Ir(III) complexes, which have been widely used to drive photoredox organic synthesis [5,104]. These d^6 octahedral metal photocatalysts initiate photochemical reactions via an outer-sphere electron transfer reaction with substrates. In most cases, a sacrificial electron donor (acceptor) is required to reduce (oxidize) the oxidized (reduced) photocatalyst to complete the catalytic cycle. Less is known about triplet emitters with metal ions having vacant coordination sites for substrate binding/activation inside the coordination sphere in the excited state (Figure 5c). For Pt(II) and Au(I) complexes (M^n), in addition to outer-sphere electron transfer, their vacant axial coordination sites allow the excited complex to engage in inner-sphere C–X (X=H, halides) bond cleavage to give a short-lived $M^{n+1}-X$ intermediate. $[\text{Pt}_2(\text{pop})_4]^{4+}$ (pop = μ -pyrophosphito) is a well-known example showing such reactivity [105]. Its $^3[5d\sigma^*6p\sigma]$ excited state with τ of 9 μs at room temperature is known to undergo inner-sphere hydrogen atom abstraction reactions with R–H bonds, including aliphatic alcohols, tributyltin hydride and 1,4-cyclohexadiene, to generate Pt^{III} -hydride species (Figure 5d). Importantly, the as-formed $[\text{Pt}^{\text{III}}_2(\text{pop})_4(\text{H})_2]^{4+}$ undergoes reductive elimination to release H_2 and regenerate the photocatalyst without the need for a sacrificial electron donor/acceptor. $[\text{Pt}_2(\text{pop-BF}_2)_4]^{4+}$, the perfluoroborated analogue of $[\text{Pt}_2(\text{pop})_4]^{4+}$ with a higher excited state reduction potential of +0.86 V vs. $\text{Cp}_2\text{Fe}^{+/0}$, has recently been demonstrated to be an efficient photocatalyst for oxidant-free acceptorless dehydrogenation of aliphatic alcohols and saturated N-heterocycles with high product yields and substrates (75 examples) present in limiting amounts [106]. In addition to binuclear complexes, a Pt(II) terpyridyl acetylide complex displaying a $^3\text{MLCT}$ excited state was reported to catalyze the dehydrogenation of Hantzsch 1,4-dihydropyridines to give hydrogen gas and pyridines via hydrogen atom abstraction [107]. A cyclometalated Pt(II) diphosphine complex was found to catalyze the photoinduced difluoroalkylation of cinnamic acids and alkynes via inner-sphere binding with ethyl difluoroiodoacetate [108]. A tetradentate Pt(II) complex with redox potentials $E[(\text{Pt}^+/\text{Pt}^*)]$ of -2.63 V and $E[(\text{Pt}^0/\text{Pt}^-)]$ of -3.05 V vs. $\text{Cp}_2\text{Fe}^{+/0}$

acted as a powerful reductant for light-induced reductive coupling of aromatic carbonyls and hydrodebromination of aryl bromides [109].

Binuclear Au(I) diphosphine complexes, particularly $[\text{Au}_2(\text{dppm})_2]^{2+}$ (dppm = bis(diphenylphosphino)methane), have also been reported to undergo photoinduced C-X bond activation via inner-sphere atom abstraction (Figure 5e). The first example is the homocoupling of benzyl chloride to give dibenzyl (up to 172 turnover numbers) with $[\text{Au}_2(\text{dppm})_2](\text{OTf})_2$ as the photocatalyst [110]. This photoinduced C-X bond activation by $[\text{Au}_2(\text{dppm})_2]^{2+*}$ has recently been harnessed for direct alkylation of heteroarenes with alkyl bromides [111]. Notably, the use of $[\text{Ir}(\text{ppy})_3]$ and $[\text{Ir}((\text{dtbbpy})_2(\text{ppy}))](\text{PF}_6)_2$ as photocatalysts did not give the expected product, highlighting the uniqueness of triplet emitters derived from coordinatively unsaturated d^8 and d^{10} metal complexes for developing charge-neutral photoredox catalysis.

Concluding Remarks

With the efforts made by both experimental and theoretical scientists over the past few decades, the research on triplet emitters has greatly improved our understanding of their photophysics and the rationale behind their properties, although there are still a number of standing issues, as highlighted below.

Most of the photoluminescence from transition metal complexes is assigned to being derived from phosphorescence, particularly for 3rd-row transition metal complexes, based on the heavy atom effect and microsecond regime emission lifetimes. However, recent works on Au(I), Au(III) and W(VI) complexes raise concerns about emission assignments based purely on emission lifetimes and the nature of metal ions, as some of these complexes display TADF as revealed by time-resolved spectroscopic and temperature-dependent emission studies and theoretical analyses. These findings call for a more careful examination of their emission origin particularly for those with k_r values of 10^5 - 10^6 s⁻¹.

With the rational ligand design insights obtained in the studies on phosphorescent transition metal complexes, significant efforts should be made to develop luminescent earth-abundant, 1st-row transition metal complexes as sustainable alternatives to precious metal photofunctional materials. Although a multitude of strongly luminescent Zn(II) and Cu(I) complexes are known, examples of iron, cobalt and nickel complexes displaying

luminescence at room temperature remain rare due to the presence of low-lying, deactivating metal-centered excited states [9,112]. By employing strong σ -donating bi/tridentate carbene ligands to impart a strong ligand field, an Fe(II) complex with a long-lived (528 ps) $^3\text{MLCT}$ excited state and an Fe(III) complex exhibiting $^2\text{LMCT}$ emission (λ_{max} : 655 nm; Φ_{PL} : 2.1%; τ : 2 ns) have recently been discovered [113,114]. These remarkable breakthroughs are envisioned to invigorate further studies that will uncover new directions and design principles for luminescent 1st-row transition metal complexes.

Glossary

Phosphorescence: a radiative electronic transition from an excited state to ground state that involves a change in spin multiplicity.

Intersystem crossing (ISC): a radiationless electronic transition process that involves a change in spin multiplicity.

Spin-selection rule: transitions between states of different spin multiplicities are spin-forbidden and not allowed.

Spin-orbit coupling: the interaction between the spin angular momentum and the orbital angular momentum.

Transition dipole moment: the transition dipole moment for a transition between states $|i\rangle$ and $|f\rangle$ is defined as $\mu_{if} = \langle i|\boldsymbol{\mu}|f\rangle$ where $\boldsymbol{\mu} = e\mathbf{r}$ is the electric dipole operator.

k_r and k_{nr} : radiative and non-radiative decay rate constants respectively.

Excimer: an excited molecular complex of definite stoichiometry of the same molecular components but is dissociated in its ground state.

MMLCT: an electronic transition from an occupied orbital that involves overlap of two metal orbitals upon forming a close metal-metal contact to a ligand-based unoccupied orbital.

Thermally activated delayed fluorescence (TADF): a process that an excited molecule in triplet manifolds absorbs the thermal energy to undergo reverse ISC from the triplet excited state to a higher-lying singlet excited state, followed by fluorescence.

Supramolecular polymerization: polymerization process driven by highly directional and reversible non-covalent interaction.

Acknowledgements

This work was supported by Guangdong Major Project of Basic and Applied Basic Research (2019B030302009), Science, Technology and Innovation Commission of Shenzhen Municipality (JCYJ20170818141858021, JCYJ20180508162429786) and the Hong Kong Research Grants Council (HKU 17330416).

References

1. Chi, Y. and Chou P.-T. (2010) Transition-Metal Phosphors with Cyclometalating Ligands: Fundamentals and Applications. *Chem. Soc. Rev.* 39, 638-655
2. You, Y. and Nam, W. (2012) Photofunctional Triplet Excited States of Cyclometalated Ir(III) Complexes: Beyond Electroluminescence. *Chem. Soc. Rev.* 41, 7061-7084
3. Xiang, H. et al. (2013) Near-Infrared Phosphorescence: Materials and Applications. *Chem. Soc. Rev.* 42, 6128-6185
4. Zhao, Q. et al. (2011) Phosphorescent Heavy-Metal Complexes for Bioimaging. *Chem. Soc. Rev.* 40, 2508-2524
5. Prier, C. K. et al. (2013) Visible Light Photoredox Catalysis with Transition Metal Complexes: Applications in Organic Synthesis. *Chem. Rev.* 113, 5322-5363
6. Tang, M.-C. et al. (2016) Platinum and Gold Complexes for OLEDs. *Top. Curr. Chem.* 374, 46
7. Förster, C. and Heinze, K. (2020) Photophysics and Photochemistry with Earth-Abundant Metals – Fundamentals and Concepts. *Chem. Soc. Rev.* 49, 1057-1070
8. Hockin, B. M. et al. (2019) Photoredox Catalysts Based on Earth-Abundant Metal Complexes. *Catal. Sci. Technol.* 9, 889-915
9. Wenger, O. S. (2019) Is Iron the New Ruthenium? *Chem. Eur. J.* 25, 6043-6052
10. Li, K. et al. (2016) Highly Phosphorescent Platinum(II) Emitters: Photophysics, Materials and Biological Applications. *Chem. Sci.* 7, 1653-1673
11. Lu, W. et al. (2004) Light-Emitting Tridentate Cyclometalated Platinum(II) Complexes Containing σ -Alkynyl Auxiliaries: Tuning of Photo- and Electrophosphorescence. *J. Am. Chem. Soc.* 126, 4958-4971
12. Yam, V. W.-W. et al. (2005) Luminescent Gold(III) Alkynyl Complexes: Synthesis, Structural Characterization, and Luminescence Properties. *Angew. Chem. Int. Ed.* 44, 3107-3110
13. Kui, S. C. F et al. (2013) Robust Phosphorescent Platinum(II) Complexes Containing Tetradentate $O^N^C^N$ Ligands: Excimeric Excited State and Application in Organic White-Light-Emitting Diodes. *Chem. Eur. J.* 19, 69-73
14. Kui, S. C. F. et al. (2013) Robust Phosphorescent Platinum(II) Complexes with Tetradentate $O^N^C^N$ Ligands: High Efficiency OLEDs with Excellent Efficiency Stability. *Chem. Commun.* 49, 1497-1499
15. Turner, E. et al. (2013) Cyclometalated Platinum Complexes with Luminescent Quantum Yields Approaching 100%. *Inorg. Chem.* 52, 7344-7351

16. Cheng, G. et al. (2014) Structurally Robust Phosphorescent [Pt(O^NC^N)] Emitters for High Performance Organic Light-Emitting Devices with Power Efficiency up to 126 lm W⁻¹ and External Quantum Efficiency over 20%. *Chem. Sci.* 5, 4819-4830
17. Chow, P.-K. et al (2013) Strongly Phosphorescent Palladium(II) Complexes of Tetradentate Ligands with Mixed Oxygen, Carbon, and Nitrogen Donor Atoms: Photophysics, Photochemistry, and Applications. *Angew. Chem. Int. Ed.* 52, 11775-11779
18. Chow, P.-K. et al (2016) Highly Luminescent Palladium(ii) Complexes with Sub-Millisecond Blue to Green Phosphorescent Excited States. Photocatalysis and Highly Efficient PSF-OLEDs. *Chem. Sci.* 7, 6083-6098
19. To, W.-P. et al. (2012) Luminescent Organogold(III) Complexes with Long-Lived Triplet Excited States for Light-Induced Oxidative C-H Bond Functionalization and Hydrogen Production. *Angew. Chem. Int. Ed.* 51, 2654-2657
20. To, W.-P. et al. (2013) Strongly Luminescent Gold(III) Complexes with Long-Lived Excited States: High Emission Quantum Yields, Energy Up-Conversion, and Nonlinear Optical Properties. *Angew. Chem. Int. Ed.* 52, 6648-6652
21. Sattler, W. et al. (2015) Bespoke Photoreductants: Tungsten Arylisocyanides. *J. Am. Chem. Soc.* 137, 1198-1205
22. Herr, P. et al. (2019) Long-Lived, Strongly Emissive, and Highly Reducing Excited States in Mo(0) Complexes with Chelating Isocyanides. *J. Am. Chem. Soc.* 141, 14394-14402
23. Büldt, L. A. et al. (2017) A Tris(diisocyanide)chromium(0) Complex is a Luminescent Analog of Fe(2,2'-Bipyridine)₃²⁺. *J. Am. Chem. Soc.* 139, 985-992
24. Larsen, C. B. and Wenger, O. S. (2018) Photophysics and Photoredox Catalysis of a Homoleptic Rhenium(I) Tris(diisocyanide) Complex. *Inorg. Chem.* 57, 2965-2968
25. Büldt, L. A. et al. (2017) Luminescent Ni⁰ Diisocyanide Chelates as Analogues of CuI Diimine Complexes. *Chem. Eur. J.* 23, 8577-8580
26. Cheng, G. et al. (2019) High-Performance Deep-Red/Near-Infrared OLEDs with Tetradentate [Pt(O^NC^N)] Emitters. *Adv. Opt. Mater.* 7, 1801452
27. Au, V. K.-M. et al. (2009) Luminescent Cyclometalated N-Heterocyclic Carbene-Containing Organogold(III) Complexes: Synthesis, Characterization, Electrochemistry, and Photophysical Studies. *J. Am. Chem. Soc.* 131, 9076-9085
28. Cheng, G. et al. (2014) Color Tunable Organic Light-Emitting Devices with External Quantum Efficiency over 20% Based on Strongly Luminescent Gold(III) Complexes having Long-Lived Emissive Excited States. *Adv. Mater.* 26, 2540-2546

29. Wong, K. M.-C. et al. (2013) Noncovalent Metal-Metal Interactions. In *Comprehensive Inorganic Chemistry II* (2nd edn) (Reedijk, J. and Poeppelemeier, K., eds), pp. 59-130. Elsevier
30. Biedermann, J. et al. (1990) Spectroscopic Studies of Cyclo-Metallated Pt(II) Complexes: Optical Absorption and Emission and the Structure of Single Crystal [Pt(bpm)(CN)₂] \cdot H₂O (bpm = 2,2'-Bipyrimidine). *Inorg. Chim. Acta* 169, 63-70
31. Biedermann, J. et al. (1990) Spectroscopic Studies of Cyclometalated Platinum(II) Complexes: Superposition of Two Difference Spectroscopic Species in the Electronic Spectra of a Single Crystal of [Pt(bpm)(CN)₂] (bpm = 2,2'-Bipyrimidine). *Inorg. Chem.* 29, 1884-1888
32. Miskowski, V. M. and Houlding V. H. (1991) Electron Spectra and Photophysics of Platinum(II) Complexes with α -Diimine Ligands. Solid-State Effects. 2. Metal-Metal Interaction in Double Salts and Linear Chains. *Inorg. Chem.* 30, 4446-4452
33. Yip, H.-K. et al. (1992) Photophysical Properties and X-ray Crystal Structure of a Luminescent Platinum(II) Dimer [Pt₂(2,2': 6',2''-terpyridine)₂(Gua)](ClO₄)₃ \cdot H₂O (Gua = guanidine anion). *J. Chem. Soc. Chem. Commun.* 1369-1371
34. Leopold, H. et al. (2016) Binuclear C[^]C* Cyclometalated Platinum(II) NHC Complexes with Bridging Amidinate Ligands. *Angew. Chem. Int. Ed.* 55, 15779-15782
35. Zhu, Y. et al. (2017) Binuclear Platinum(II) Complexes Based on 2-mercaptobenzothiazole 2-Mercaptobenzimidazole and 2-Hydroxypyridine as Bridging Ligands: Red and Near-Infrared Luminescence Originated from MMLCT Transition. *Dyes Pigm.* 145, 144-151
36. Ly, K. T. et al. (2017) Near-Infrared Organic Light-Emitting Diodes with Very High External Quantum Efficiency and Radiance. *Nat. Photonics* 11, 63-68
37. Wan, Q. et al (2018) The Metal–Metal-to-Ligand Charge Transfer Excited State and Supramolecular Polymerization of Luminescent Pincer Pd^{II}–Isocyanide Complexes. *Angew. Chem. Int. Ed.* 57, 3089-3093
38. Lin, J. et al. (2019) Highly Phosphorescent Organopalladium(II) Complexes with Metal–Metal-to-Ligand Charge-Transfer Excited States in Fluid Solutions. *Dalton Trans.* 48, 10417-10421
39. Wan, Q. et al. (2019) Kinetically Controlled Self-Assembly of Phosphorescent Au^{III} Aggregates and Ligand-to-Metal–Metal Charge Transfer Excited State: A Combined Spectroscopic and DFT/TDDFT Study. *J. Am. Chem. Soc.* 141, 11572-11582

40. Czerwieniec, R. et al. (2011) Blue-Light Emission of Cu(I) Complexes and Singlet Harvesting. *Inorg. Chem.* 50, 8293-8301
41. Endo, A. et al. (2009) Thermally Activated Delayed Fluorescence from Sn⁴⁺-Porphyrin Complexes and Their Application to Organic Light Emitting Diodes – A Novel Mechanism for Electroluminescence. *Adv. Mater.* 21, 4802-4806
42. Yersin, H. et al. (2017) TADF Material Design: Photophysical Background and Case Studies Focusing on Cu^I and Ag^I Complexes. *ChemPhysChem* 18, 3508-3535
43. Li, G. et al (2019) Metal Complex Based Delayed Fluorescence Materials. *Org. Electron.* 69, 135-152
44. Hamze, R. et al. (2019) Eliminating Nonradiative Decay in Cu(I) Emitters: >99% Quantum Efficiency and Microsecond Lifetime. *Science* 363, 601-606
45. Schinabeck, A. et al. (2019) Symmetry-Based Design Strategy for Unprecedentedly Fast Decaying Thermally Activated Delayed Fluorescence (TADF). Application to Dinuclear Cu(I) Compounds. *Chem. Mater.* 31, 4392-4404
46. Di, D. et al. (2017) High-Performance Light-Emitting Diodes Based on Carbene-Metal-Amides. *Science* 356, 159-163
47. Conaghan, P. J. et al (2018) Efficient Vacuum-Processed Light-Emitting Diodes Based on Carbene-Metal-Amides. *Adv. Mater.* 30, 1802285
48. Föllner, J. and Marian, C. M. (2017) Rotationally Assisted Spin-State Inversion in Carbene–Metal–Amides Is an Artifact. *J. Phys. Chem. Lett.* 8, 5643-5647
49. Zhu, Z.-Q. et al. (2015) Harvesting All Electrogenenerated Excitons through Metal Assisted Delayed Fluorescent Materials. *Adv. Mater.* 27, 2533-2537
50. Zhu, Z.-Q. et al. (2019) Highly Efficient Blue OLEDs Based on Metal-Assisted Delayed Fluorescence Pd(II) Complexes. *Adv. Opt. Mater.* 7, 1801518
51. Fernandez-Cestau, J. et al. (2015) Synthesis and Luminescence Modulation of Pyrazine-Based Gold(III) Pincer Complexes. *Chem. Commun.* 51, 16629-16632
52. To, W.-P. et al. (2017) Highly Luminescent Pincer Gold(III) Aryl Emitters: Thermally Activated Delayed Fluorescence and Solution-Processed OLEDs. *Angew. Chem. Int. Ed.* 56, 14036-14041
53. Zhou, D. et al. (2019) Thermally Stable Donor–Acceptor Type (Alkynyl)Gold(III) TADF Emitters Achieved EQEs and Luminance of up to 23.4% and 70 300 cd m⁻² in Vacuum-Deposited OLEDs. *Adv. Sci.* 6, 1802297

54. Zhou, D. et al. (2020) Tetradentate Gold(III) Complexes as Thermally Activated Delayed Fluorescence (TADF) Emitters: Microwave-Assisted Synthesis and High-Performance OLEDs with Long Operational Lifetime. *Angew. Chem. Int. Ed.* 59, 6375-6382
55. Li, L.-K. et al. (2019) Strategies Towards Rational Design of Gold(III) Complexes for High-Performance Organic Light-Emitting Devices. *Nat. Photonics* 13, 185-191
56. Chan, K.-T. et al. (2019) Strongly Luminescent Tungsten Emitters with Emission Quantum Yields of up to 84 %: TADF and High-Efficiency Molecular Tungsten OLEDs. *Angew. Chem. Int. Ed.* 58, 14896-14900
57. Juliá, F. et al. (2014) Homoleptic Tris-Cyclometalated Platinum(IV) Complexes: a New Class of Long-Lived, Highly Efficient ³LC Emitters. *Chem. Sci.* 5, 1875-1880
58. Kumar, R. et al. (2015) Luminescent (N[^]C[^]C) Gold(III) Complexes: Stabilized Gold(III) Fluorides. *Angew. Chem. Int. Ed.* 54, 14287-14290
59. Bachmann, M et al. (2017) Harnessing White-light Luminescence via Tunable Singlet- and Triplet-Derived Emissions Based on Gold(III) Complexes. *Chem. Eur. J.* 23, 9451-9456
60. Malmberg, R. et al. (2019) Thermally Robust and Tuneable Phosphorescent Gold(III) Complexes Bearing (N[^]N)-type Bidentate Ligands as Ancillary Chelates. *Chem. Eur. J.* 25, 3627-3636
61. Tang, M.-C. et al. (2019) Rational Molecular Design for Realizing High Performance Sky-Blue-Emitting Gold(III) Complexes with Monoaryl Auxiliary Ligands and Their Applications for Both Solution-Processable and Vacuum-Deposited Organic Light-Emitting Devices. *Chem. Sci.* 10, 594-605
62. Cui, X. et al. (2016) Accessing the Long-Lived Triplet Excited States in Transition-Metal Complexes: Molecular Design Rationales and Applications. *Chem. Rec.* 16, 173-188
63. Castellano, F. N. (2015) Altering Molecular Photophysics by Merging Organic and Inorganic Chromophores. *Acc. Chem. Res.* 48, 828-839
64. Kui, S. C. F. et al. (2012) Luminescent Organoplatinum(II) Complexes with Functionalized Cyclometalated C[^]N[^]C Ligands: Structures, Photophysical Properties, and Material Applications. *Chem. Eur. J.* 18, 96-109
65. Wan, S. and Lu, W. (2017) Reversible Photoactivated Phosphorescence of Gold(I) Arylethynyl Complexes in Aerated DMSO Solutions and Gels. *Angew. Chem. Int. Ed.* 56, 1784-1788

66. Wan, S. et al. (2018) Photochemically Deoxygenating Solvents for Triplet–Triplet Annihilation Photon Upconversion Operating in Air. *Chem. Commun.* 54, 3907-3910
67. Lin, J. et al. (2019) Photo-Writing Self-Erasable Phosphorescent Images Using Poly(N-vinyl-2-pyrrolidone) as a Photochemically Deoxygenating Matrix. *Chem. Commun.* 55, 4299-4302
68. Wan, S. et al. (2020) A Prototype of Volumetric Three-Dimensional Display Based on Programmable Photo-activated Phosphorescence. *Angew. Chem. Int. Ed.* DOI: 10.1002/anie.202003160
69. Yam, V. W.-W. et al. (2015) Light-Emitting Self-Assembled Materials Based on d8 and d10 Transition Metal Complexes. *Chem. Rev.* 115, 7589-7728
70. Gao, Z. et al. (2018) Multicomponent Assembled Systems Based on Platinum(II) Terpyridine Complexes. *Acc. Chem. Res.* 51, 2719-2729
71. Che, C.-M. et al (2003) Solvatochromic Response Imposed by Environmental Changes in Matrix/Chromophore Entities: Luminescent Cyclometalated Platinum(II) Complex in Nafion and Silica Materials. *Chem. Commun.* 118-119
72. Lu, W. et al. (2009) Supramolecular Polymers and Chromonic Mesophases Self-Organized from Phosphorescent Cationic Organoplatinum(II) Complexes in Water. *Angew. Chem. Int. Ed.* 48, 7621-7625
73. Zhang, K. et al. (2017) Living Supramolecular Polymerization Achieved by Collaborative Assembly of Platinum(II) Complexes and Block Copolymers. *Proc. Natl Acad. Sci. USA* 114, 11844–11849
74. Aliprandi, A. et al. (2016) Controlling and Imaging Biomimetic Self-Assembly. *Nat. Chem.* 8, 10-15
75. Robinson, M. E. et al. (2017) Dimensional Control and Morphological Transformations of Supramolecular Polymeric Nanofibers Based on Cofacially-Stacked Planar Amphiphilic Platinum(II) Complexes. *ACS Nano* 11, 9162-9175
76. Li, Z. et al. (2017) Supramolecular Engineering of Discrete Pt(II)···Pt(II) Interactions for Visible-Light Photocatalysis. *ACS Catal.* 7, 4676-4681
77. Yuen, M.-Y. et al. (2008) Semiconducting and Electroluminescent Nanowires Self-Assembled from Organoplatinum(II) Complexes. *Angew. Chem. Int. Ed.* 47, 9895-9899
78. Che, C.-M. et al. (2011) Single Microcrystals of Organoplatinum(II) Complexes with High Charge-Carrier Mobility. *Chem. Sci.* 2, 216-220

79. Lai, S.-W. et al. (1999) Synthesis of Organoplatinum Oligomers by Employing N-Donor Bridges with Predesigned Geometry: Structural and Photophysical Properties of Luminescent Cyclometalated Platinum(II) Macrocycles. *Organometallics* 18, 3991-3997
80. Ma, B. et al. (2005) Synthetic Control of Pt-Pt Separation and Photophysics of Binuclear Platinum Complexes. *J. Am. Chem. Soc.* 127, 28-29
81. Zhou, C. et al. (2015) Precise Design of Phosphorescent Molecular Butterflies with Tunable Photoinduced Structural Change and Dual Emission. *Angew. Chem. Int. Ed.* 54, 9591-9595
82. Han, M. et al. (2014) A Phosphorescent Molecular "Butterfly" That Undergoes a Photoinduced Structural Change Allowing Temperature Sensing and White Emission. *Angew. Chem. Int. Ed.* 53, 10908-10912
83. Lai, S.-W. et al. (1998) [$\{\text{Pt}(\text{CN})(\text{C}_{10}\text{H}_{21}\text{N}_4)\}_6$]: A Luminescent Hexanuclear Platinum(ii) Macrocycle Containing Chelating Dicarbene and Bridging Cyanide Ligands. *Angew. Chem. Int. Ed.* 37, 182-184
84. Lai, S.-W. et al. (1999) Self-Assembly of Predesigned Trimetallic Macrocycles Based on Benzimidazole as Nonlinear Bridging Motifs: Crystal Structure of a Luminescent Platinum(II) Cyclic Trimer. *Angew. Chem. Int. Ed.* 38, 669-671
85. Yan, X. et al. (2015) Highly Emissive Platinum(II) Metallacages. *Nat. Chem.* 7, 342-348
86. Liu, N. et al. (2019) Suite of Organoplatinum(II) Triangular Metallaprism: Aggregation-Induced Emission and Coordination Sequence Induced Emission Tuning. *J. Am. Chem. Soc.* 141, 9448-9452
87. Mukherjee S. and Mukherjee P. S. (2014) Template-Free Multicomponent Coordination-Driven Self-Assembly of Pd(II)/Pt(II) Molecular Cages. *Chem. Commun.* 50, 2239-2248
88. Cook, T. R. and Stang, P. J. (2015) Recent Developments in the Preparation and Chemistry of Metallacycles and Metallacages via Coordination. *Chem. Rev.* 115, 7001-7045
89. Ma, D.-L. et al. (2012) Recent Advances in Luminescent Heavy Metal Complexes for Sensing. *Coord. Chem. Rev.* 256, 3087-3113
90. Pierre, V. C. et al. (2007) Insights into Finding a Mismatch through the Structure of a Mismatched DNA Bound by a Rhodium Intercalator. *Proc. Natl. Acad. Sci. U.S.A.* 104, 429-434
91. Song, H. et al. (2012) Crystal Structure of Δ -[Ru(bpy)₂dppz]²⁺ Bound to Mismatched DNA Reveals Side-by-Side Metalloinsertion and Intercalation. *Nat. Chem.* 4, 615-620

92. Liu, H.-Q. et al. (1995) Interaction of a Luminescent Platinum(II) Complex of Substituted 2,2'-Bipyridine with DNA. Spectroscopic and Photophysical Studies. *Chem. Commun.* 509-510
93. Zou, T. et al. (2014) Luminescent Cyclometalated Platinum(II) Complex Forms Emissive Intercalating Adducts with Double-Stranded DNA and RNA: Differential Emissions and Anticancer Activities. *Angew. Chem. Int. Ed.* 53, 10119-10123
94. Fung, S. K. et al. (2016) Luminescent Platinum(II) Complexes with Functionalized N-Heterocyclic Carbene or Diphosphine Selectively Probe Mismatched and Abasic DNA. *Nat. Commun.* 7, 10655
95. Baggaley, E. et al. (2012) Lighting the Way to See Inside the Live Cell with Luminescent Transition Metal Complexes. *Coord. Chem. Rev.* 256, 1762-1785
96. Zhang, K. Y. et al. (2018) Long-Lived Emissive Probes for Time-Resolved Photoluminescence Bioimaging and Biosensing. *Chem. Rev.* 118, 1770-1839
97. Yoshihara, T. et al. (2012) Ratiometric Molecular Sensor for Monitoring Oxygen Levels in Living Cells. *Angew. Chem. Int. Ed.* 51, 4148-4151
98. Zhao, Q et al. (2015) Fluorescent/Phosphorescent Dual-Emissive Conjugated Polymer Dots for Hypoxia Bioimaging. *Chem. Sci.* 6, 1825-1829
99. Tsai, J. L.-L. et al. (2015) Luminescent Platinum(II) Complexes with Self-Assembly and Anti-Cancer Properties: Hydrogel, pH Dependent Emission Color and Sustained-Release Properties under Physiological Conditions. *Chem. Sci.* 6, 3823-3830
100. Wong, K. M.-C. and Yam, V. W.-W. (2007) Luminescence Platinum(II) Terpyridyl Complexes – from Fundamental Studies to Sensory Functions. *Coord. Chem. Rev.* 251, 2477-2488
101. Wong, K. M.-C. and Yam, V. W.-W. (2011) Self-Assembly of Luminescent Alkynylplatinum(II) Terpyridyl Complexes: Modulation of Photophysical Properties through Aggregation Behavior. *Acc. Chem. Res.* 44, 424-434
102. Yeung, M. C.-L. and Yam, V. W.-W. (2015) Luminescent Cation Sensors: from Host–Guest Chemistry, Supramolecular Chemistry to Reaction-Based Mechanisms. *Chem. Soc. Rev.* 44, 4192-4202
103. Chung, C. Y.-S. and Yam, V. W.-W. (2011) Induced Self-Assembly and Förster Resonance Energy Transfer Studies of Alkynylplatinum(II) Terpyridine Complex Through Interaction With Water-Soluble Poly(phenylene ethynylene sulfonate) and the Proof-of-Principle Demonstration of this Two-Component Ensemble for Selective Label-Free Detection of Human Serum Albumin. *J. Am. Chem. Soc.* 133, 18775-18784

104. McAtee, R. C. et al. (2019) Illuminating Photoredox Catalysis. *Trends Chem.* 1, 111-125
105. Roundhill, D. M. et al. (1989) Pyrophosphito-Bridged Diplatinum Chemistry. *Acc. Chem. Res.* 22, 55-61
106. Zhong, J.-J. et al. (2019) Efficient Acceptorless Photo-Dehydrogenation of Alcohols and N-Heterocycles with Binuclear Platinum(II) Diphosphite Complexes. *Chem. Sci.* 10, 4883-4889
107. Zhang, D. et al. (2004) Photocatalytic Hydrogen Production from Hantzsch 1,4-Dihydropyridines by Platinum(II) Terpyridyl Complexes in Homogeneous Solution. *J. Am. Chem. Soc.* 126, 3440-3441
108. Zhong, J.-J. et al. (2017) Platinum(II) Photo-Catalysis for Highly Selective Difluoroalkylation Reactions. *Chem. Commun.* 53, 8948-8951
109. Li, K. et al. (2018) Air-Stable Blue Phosphorescent Tetradentate Platinum(II) Complexes as Strong Photo-Reductant. *Angew. Chem. Int. Ed.* 57, 14129-14133
110. Li, D. et al. (1992) Photoinduced C–C Bond Formation from Alkyl Halides Catalysed by Luminescent Dinuclear Gold(I) and Copper(I) Complexes. *J. Chem. Soc., Dalton Trans.* 3325-3329
111. McCallum, T. and Barriault, L. (2016) Direct Alkylation of Heteroarenes with Unactivated Bromoalkanes using Photoredox Gold Catalysis. *Chem. Sci.* 7, 4754-4758
112. Büldt, L. A. and Wenger, O. S. (2017) Chromium(0), Molybdenum(0), and Tungsten(0) Isocyanide Complexes as Luminophores and Photosensitizers with Long-Lived Excited States. *Angew. Chem. Int. Ed.* 56, 5676-5682
113. Chábera, P. et al. (2018) Fe^{II} Hexa N-Heterocyclic Carbene Complex with a 528 ps Metal-to-Ligand Charge-Transfer Excited-State Lifetime. *J. Phys. Chem. Lett.* 9, 459-463
114. Kjær, K. S. et al. (2019) Luminescence and Reactivity of a Charge-Transfer Excited Iron Complex with Nanosecond Lifetime. *Science* 363, 249-253